Low Complexity Joint Detection and Estimation for MIMO RIS-ISAC Systems

Nathanael Danso-Ntiamoah, *Graduate Student Member, IEEE,* Aseni Jayarathne, *Graduate Student Member, IEEE* Ibrahim Al-Nahhal, *Senior Member, IEEE,* Octavia A. Dobre, *Fellow, IEEE,* Hyundong Shin, *Fellow, IEEE*

***Abstract*—Integrated sensing and communications (ISAC) and reconfigurable intelligent surfaces (RIS) have been identified as key technologies in the realization of next-generation wireless networks. ISAC provides spectral and hardware efficiency by integrating the communications and sensing functionalities into one system, whilst RIS is used to improve signal transmission. In this letter, a low-cost RIS-ISAC receiver is proposed for the first time in a multiple-input multiple-output (MIMO) system. A search-tree is deployed to detect the MIMO RIS-ISAC transmitted communication signals. Next, the K-best algorithm is proposed to reduce the computational complexity of maximum likelihood (ML) detection while achieving near-ML bit-error rate performance. Additionally, the minimum mean-squared error estimation technique is adopted to estimate the reflection coefficients of a nearby target. Computational complexity analysis and Monte Carlo simulations are provided to support the findings.**

***Index Terms*—Integrated sensing and communications (ISAC), reconfigurable intelligent surfaces (RIS), K-best algorithm, multiple-input multiple-output (MIMO), complexity analysis.**

I. Introduction

NEXT-generation networks are considered key enablers for applications such as ubiquitous Internet-of-things, autonomous driving, smart cities, and virtual reality. Many of these emerging applications require environment/location-related information in their operation, achieved through sensing and enhanced connectivity to transmit the sensory information. Integrated sensing and communications (ISAC) is an emerging technology that seeks to merge the communications and sensing functionalities into one block to achieve a more spectrally efficient system [1].

Despite the potential of ISAC systems, the stochastic property of the wireless channel remains an undesired characteristic. Obstacles in the environment that randomly scatter or reflect electromagnetic waves present an inherent unreliability in the channel. This random behavior of the wireless channel, if not mitigated, can severely impair the performance of the communication system. In recent years, reconfigurable intelligent surfaces (RIS) have risen to prominence as a technology to mitigate the effects of the random behavior of the wireless channel [2], [3]. By correctly characterizing the wireless channel, an optimized RIS can be used to achieve the desired reflection of the electromagnetic waves and improve the overall performance of a wireless communication system.

While research in RIS-ISAC systems remain state-of-the-art, a significant number of the studies that have been carried out in this area focused on beamforming design [4], [5] and optimizing the phase shift of the RIS [6], [7]. Additionally, a simultaneously transmitting and reflecting RIS-aided ISAC scheme was proposed to simultaneously enhance an in-vehicle user equipment (UE) communication and sense the vehicle [8]. Nonetheless, to the best of our knowledge, no existing work has explored the design of a joint receiver for RIS-ISAC systems. The design objective of the joint RIS-ISAC receiver is to simultaneously recover the transmitted communication symbols and estimate the presence of a nearby target with minimal errors. A theoretical joint ISAC receiver was proposed in [9], in which maximum likelihood (ML) detection was used to detect the communication symbols in a single-input multiple-output (SIMO) system, while the minimum mean square error (MMSE) estimator was used to estimate the target coefficients in an interference cancellation (IC) technique.

Although ML detection offers theoretically optimum performance, its complexity scales exponentially with the number of transmit antennas in a multiple-input multiple-output (MIMO) system. Motivated by the prohibitive complexity of ML detection and compared to [9] that studies a SIMO ISAC system, this work considers a reduced complexity detection algorithm for a MIMO RIS-ISAC system to address the complexity bottleneck arising from a higher number of antennas and a cascaded channel. The contributions of this paper are:

- First-time investigation of a reliable joint receiver for an optimized-phase shift RIS-ISAC system in the literature.
- System model reformulation to efficiently use a search-tree (ST) approach in detecting communication symbols.
- First-time application of the K-best algorithm (KBA) in the ST technique in a MIMO RIS-ISAC system to achieve near-optimal performance with reduced computational complexity and greater degrees of freedom.
- Adopting the IC technique from [9] to estimate the coefficients of a target in the MIMO RIS-ISAC system.
- Deriving general formulas for the complexity in terms of the number of real additions (RA) and real multiplications (RM) involved in the proposed KBA.
- Providing Monte Carlo simulations to verify the findings.

This work was supported by the Canada Research Chairs Program CRC-2022-00187. (*Nathanael Danso-Ntiamoah and Aseni Jayarathne contributed equally to this manuscript.*) *Corresponding authors: Octavia A. Dobre; Hyundong Shin.*

Nathanael Danso-Ntiamoah, Aseni Jayarathne, Ibrahim Al-Nahhal and Octavia A. Dobre are with the Faculty of Engineering and Applied Science, Memorial University, St. John's, NL A1C 5S7, Canada (e-mail: ndansontiamoah@mun.ca; acjayarathne@mun.ca; ioalnahhal@mun.ca; odobre@mun.ca). Octavia A. Dobre is also with Kyung Hee University, South Korea.

Hyundong Shin is with the Department of Electronics and Information Convergence Engineering, Kyung Hee University, Yongin 17104, South Korea (email: hshin@khu.ac.kr).

II. System Model

The system model investigated in this paper is presented in Fig. 1. A full-duplex base station (BS) with N_{ts} transmit antennas and N_r receive antennas is considered, using uniform linear array (ULA) with antennas spaced at the half-wavelength distance. For simplicity, we assume that self-interference is canceled at the full-duplex ISAC BS before processing the joint received signal [10]. The ISAC BS jointly receives the uplink communication signals from a UE with N_{tu} transmit antennas and the echoes from the reflection of the sensing signal by the target. It is assumed that $N_r \geq N_{tu}$ to avoid an under-determined system. Due to the rich scattering environment in the direct UE-BS channel, an RIS is employed to provide virtual line-of-sight (LoS) links and enhance the quality of signal transmission [11].

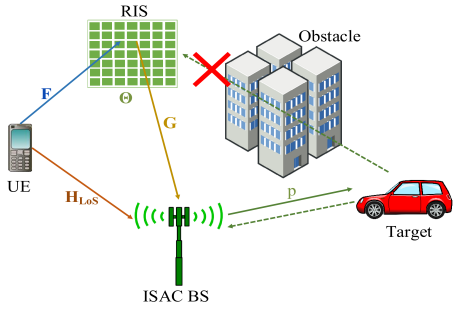

Fig. 1: The MIMO RIS-ISAC system model.

Denoting $\mathbf{x} \in \mathbb{C}^{N_{tu}\times 1}$ as the UE transmitted signal drawn from the symbols of an M-quadrature amplitude modulation (QAM) constellation, where M is a square number, then the communication signal received at the ISAC BS comprising both LoS signals and the reflected signals from N RIS elements, $\mathbf{c} \in \mathbb{C}^{N_r\times 1}$ is expressed as

$$\mathbf{c} = \sqrt{P_c}\left(\mathbf{H_{LoS}} + \mathbf{G\Theta F}\right)\mathbf{x} + \mathbf{w}_c, \tag{1}$$

where P_c is the total transmitted communication signal power. $\mathbf{H_{LoS}} \in \mathbb{C}^{N_r\times N_{tu}}$ is the UE-BS Rayleigh fading channel (i.e., $\mathbf{H_{LoS}} \sim \mathcal{CN}(0,1)$), whilst $\mathbf{F} \in \mathbb{C}^{N\times N_{tu}}$ and $\mathbf{G} \in \mathbb{C}^{N_r\times N}$ are the virtual UE-RIS and RIS-BS LoS channels respectively. $\mathbf{\Theta} = \text{diag}(e^{j\theta_1}, \cdots, e^{j\theta_n}, \cdots, e^{j\theta_N}) \in \mathbb{C}^{N\times N}$ is a diagonal matrix that represents the RIS phase shifts, where $\theta_n \in [-\pi, \pi)$ is the phase shift introduced by the n-th RIS reflecting element. The RIS phase shifts are optimized using the alternate optimization technique [12]. $\mathbf{w}_c \in \mathbb{C}^{N_r\times 1}$ is the additive white Gaussian noise (AWGN) term for the communication signal with zero-mean and variance $0.5\sigma^2$. σ^2 is the total noise power of the MIMO RIS-ISAC system.

Similarly, the sensing signal transmitted by the ISAC BS is denoted by p. To avoid the sensing signal interfering with the RIS component of the communication signal, it is assumed that the RIS is placed close to the UE, and an obstacle blocks the target echoes from impinging the RIS, as shown in Fig. 1. The sensing signal received by the ISAC BS, $\mathbf{s} \in \mathbb{C}^{N_r\times 1}$ is

$$\mathbf{s} = \sqrt{P_s}\zeta\mathbf{r}(\phi)\mathbf{t}^{\text{H}}(\phi)\mathbf{b}\text{p} + \mathbf{w}_s, \tag{2}$$

where P_s is the total transmitted sensing signal power and $(\cdot)^{\text{H}}$ is the Hermitian transpose operator. ϕ is the angle of the target in radians. ζ represents the target reflection coefficients. Following [9] and case II of the Swerling target model [13], it is assumed that the target's reflection coefficient fluctuates from one pulse to another, exhibiting an amplitude distribution that follows a Rayleigh distribution. Based on this assumption, $\zeta \sim \mathcal{CN}(0,1)$ is modeled as an independent and identically distributed (i.i.d) random variable. $\mathbf{b} \in \mathbb{C}^{N_{ts}\times 1}$ is the beamforming vector. $\mathbf{w}_s \in \mathbb{C}^{N_r\times 1}$ is the AWGN for the sensing signal with zero-mean and variance $0.5\sigma^2$, being independent of $\mathbf{w}_c$. $\mathbf{t}(\phi) \in \mathbb{C}^{N_{ts}\times 1}$ and $\mathbf{r}(\phi) \in \mathbb{C}^{N_r\times 1}$ are the transmit and receive steering vectors, respectively, given by [14]

$$\mathbf{t}(\phi) = \left[1, e^{j\frac{2\pi d}{\lambda}\sin(\phi)}, \cdots, e^{j\frac{2\pi d}{\lambda}(N_{ts}-1)\sin(\phi)}\right]^{\text{T}}, \tag{3}$$

and

$$\mathbf{r}(\phi) = \left[1, e^{j\frac{2\pi d}{\lambda}\sin(\phi)}, \cdots, e^{j\frac{2\pi d}{\lambda}(N_r-1)\sin(\phi)}\right]^{\text{T}}. \tag{4}$$

Here, $(\cdot)^{\text{T}}$ is the transpose operator, d is the separation between the elements of the ULA, and λ is the signal wavelength. It is also assumed that the radar is perfectly locked on the target, in which case $\mathbf{b} = \mathbf{t}(\phi)$. The joint received signal at the ISAC BS, $\mathbf{y} \in \mathbb{C}^{N_r\times 1}$ can be written as

$$\begin{aligned}\mathbf{y} &= \mathbf{c} + \mathbf{s} + \mathbf{w}\\ &= \sqrt{P_c}\left(\mathbf{H_{LoS}} + \mathbf{G\Theta F}\right)\mathbf{x} + \sqrt{P_s}\zeta\mathbf{r}(\phi)\mathbf{t}^{\text{H}}(\phi)\mathbf{b}\text{p} + \mathbf{w},\end{aligned} \tag{5}$$

where $\mathbf{w} = \mathbf{w}_c + \mathbf{w}_s$ and $\mathbf{w} \sim \mathcal{CN}(0, \sigma^2)$. By adopting the IC technique proposed in [9], the communication signal is first processed, in which $\mathbf{s}$ and $\mathbf{w}$ are considered as interference and noise signals, respectively. Thus, (5) becomes

$$\mathbf{y} = \sqrt{P_c}\left(\mathbf{H_{LoS}} + \mathbf{G\Theta F}\right)\mathbf{x} + \mathbf{v}, \tag{6}$$

where $\mathbf{v} = \sqrt{P_s}\zeta\mathbf{r}(\phi)\mathbf{t}^{\text{H}}(\phi)\mathbf{b}\text{p} + \mathbf{w}$. It can be noticed that $\mathbf{v}$ arises due to a linear combination of ζ and $\mathbf{w}$. Thus, $\mathbf{v}$ also has a zero-mean Gaussian distribution. Assuming perfect knowledge of the channel state information at the receiver, the ML detection problem is formulated as

$$\begin{aligned}\hat{\mathbf{x}}_{\text{ML}} = \arg\min &\|\mathbf{y} - \mathbf{H}\mathbf{x}\|^2\\ \text{s.t.} \quad &\mathbf{x} \in \mathbb{A}^{N_{tu}},\end{aligned} \tag{7}$$

where $\mathbf{H} = \sqrt{P_c}\left(\mathbf{H_{LoS}} + \mathbf{G\Theta F}\right)$ and $\mathbb{A}^{N_{tu}}$ represents the set of all realizations of the complex-valued transmitted symbols.

After detecting the communication symbol, the MMSE technique in [9] is extended to estimate the target's reflection coefficients from the received echoes in the MIMO RIS-ISAC system. Using this technique, the detected communication signal is subtracted from $\mathbf{y}$ to obtain an estimate of the target's echoes received by the ISAC BS, $\mathbf{y_s} \in \mathbb{C}^{N_r\times 1}$ as

$$\begin{aligned}\mathbf{y_s} &= \mathbf{y} - \sqrt{P_c}\left(\mathbf{H_{LoS}} + \mathbf{G\Theta F}\right)\hat{\mathbf{x}}_{\text{ML}}\\ &= \sqrt{P_s}\zeta\mathbf{r}(\phi)\mathbf{t}^{\text{H}}(\phi)\mathbf{b}\text{p} + \mathbf{w} + \Delta,\end{aligned} \tag{8}$$

where $\Delta = \mathbf{H}(\mathbf{x} - \hat{\mathbf{x}}_{\text{ML}})$. Considering that $\hat{\mathbf{x}}_{\text{ML}} \to \mathbf{x}$ in practical communication signal to interference plus noise ratio (SINR) regime, the effect of Δ on $\mathbf{y_s}$ in the presence of RIS can be assumed negligible. Hence, using the MMSE technique, the Bayesian linear problem in (8) is solved as

$$\hat{\zeta}_{\text{MMSE}} = \mathbf{q}^{\text{H}}\left[\mathbf{q}^{\text{H}}\mathbf{q} + \sigma^2\mathbf{I}\right]^{-1}\mathbf{y}_s, \tag{9}$$

where $\mathbf{q} \in \mathbb{C}^{N_r\times 1} = \sqrt{P_s}\mathbf{r}(\phi)\mathbf{t}^{\text{H}}(\phi)\mathbf{b}$. The received communication SINR is defined as

$$\text{SINR}_C = 10\log_{10}\left(\frac{\mathbb{E}\left\{P_c|\mathbf{H_{LoS}} + \mathbf{G\Theta F}|^2\right\}}{\mathbb{E}\left\{P_s|\zeta\mathbf{r}(\phi)\mathbf{t}^{\text{H}}(\phi)\mathbf{b}p|^2\right\} + \sigma^2}\right) \text{dB}. \tag{10}$$

III. Proposed K-Best Algorithm

KBA was initially proposed in [15] to address the high computational cost of ML detection in MIMO systems, which scales exponentially with the number of transmit antennas and the modulation order. As a breadth-first-based lattice decoding algorithm, the KBA seeks the best distance path in the forward direction and retains the K minimum metric nodes at each level of the sub-lattice. All other nodes that do not meet this K-best criterion are discarded. This principle ensures a constant decoding complexity. On one hand, although K should be sufficiently large enough to achieve near ML performance, this increases the computational complexity. On the other hand, reducing K minimizes the complexity and degrades the performance. Thus, it is necessary to find the value of K that achieves an optimal trade-off between the performance and complexity. In contrast to MIMO systems, MIMO RIS-ISAC systems present a more complex challenge at the receiver because of the interfering sensing signal and the cascaded channel due to the RIS. To adopt the KBA for this problem, the system model should first be reformulated.

A. MIMO RIS-ISAC System Reformulation

Let $n = 2N_r$ and $m = 2N_{tu}$. To solve (7) using an ST approach, (7) can be reformulated as

$$\dot{\mathbf{y}} = \dot{\mathbf{H}}\dot{\mathbf{x}} + \dot{\mathbf{v}}$$
$$\begin{bmatrix} \mathfrak{Re}\{\mathbf{y}\} \\ \mathfrak{Im}\{\mathbf{y}\} \end{bmatrix} = \begin{bmatrix} \mathfrak{Re}\{\mathbf{H}\} & -\mathfrak{Im}\{\mathbf{H}\} \\ \mathfrak{Im}\{\mathbf{H}\} & \mathfrak{Re}\{\mathbf{H}\} \end{bmatrix} \begin{bmatrix} \mathfrak{Re}\{\mathbf{x}\} \\ \mathfrak{Im}\{\mathbf{x}\} \end{bmatrix} + \begin{bmatrix} \mathfrak{Re}\{\mathbf{v}\} \\ \mathfrak{Im}\{\mathbf{v}\} \end{bmatrix}, \tag{11}$$

where $\dot{\mathbf{y}} \in \mathbb{R}^{n\times 1}$, $\dot{\mathbf{v}} \in \mathbb{R}^{n\times 1}$, $\dot{\mathbf{H}} \in \mathbb{R}^{n\times m}$, and $\dot{\mathbf{x}} \in \mathbb{R}^{m\times 1}$. $\mathfrak{Re}(\cdot)$ and $\mathfrak{Im}(\cdot)$ represent the real and imaginary parts, respectively. Due to this real-valued reformulation, the symbols of $\dot{\mathbf{x}}$ belong to a $\sqrt{M}$-pulse-amplitude modulation (PAM) scheme. $\dot{\mathbf{H}}$ is QR-decomposed as $\dot{\mathbf{H}} = \mathbf{QR}$, where $\mathbf{Q} \in \mathbb{R}^{n\times n}$ is a unitary matrix and $\mathbf{R} \in \mathbb{R}^{n\times m}$ is an upper triangular matrix. It should be noted that coefficients of $\mathbf{H}$ are i.i.d, which leads to $\dot{\mathbf{H}}$ being full rank. Thus, a left-multiplication of (11) by $\mathbf{Q}^{\mathrm{H}}$ yields

$$\tilde{\mathbf{y}} = \mathbf{R}\dot{\mathbf{x}} + \tilde{\mathbf{v}}, \tag{12}$$

where $\tilde{\mathbf{y}} \in \mathbb{R}^{n\times 1} = \mathbf{Q}^{\mathrm{H}}\dot{\mathbf{y}}$ and $\tilde{\mathbf{v}} \in \mathbb{R}^{n\times 1} = \mathbf{Q}^{\mathrm{H}}\dot{\mathbf{v}}$. Due to the upper triangular property of $\mathbf{R}$, (7) simplifies to [16], [17]

$$\begin{aligned} \hat{\mathbf{x}}_{\mathrm{ML}} &= \arg\min \sum_{a=1}^{m} \left| \tilde{y}_a - \sum_{b=a}^{m} r_{a,b}\dot{x}_b \right|^2 \\ &= \arg\min \left(|\tilde{y}_m - r_{m,m}\dot{x}_m|^2 + \left| \tilde{y}_{m-1} - \sum_{b=m-1}^{m} r_{m-1,b}\dot{x}_b \right|^2 \right. \\ &\quad \left. + \cdots + \left| \tilde{y}_1 - \sum_{b=1}^{m} r_{1,b}\dot{x}_b \right|^2 \right) \\ &\quad \text{s.t.} \quad \dot{x} \in \Omega, \end{aligned} \tag{13}$$

where $\tilde{y}_a$ represents the a-th element of vector $\tilde{\mathbf{y}}$, $r_{a,b}$ denotes the (a,b)-th entry of $\mathbf{R}$, and $\dot{x}_b$ represents the b-th element of $\dot{\mathbf{x}}$. Ω is the set of symbols of a $\sqrt{M}$-PAM scheme. From (13), it is possible to represent (7) by an ST with m levels with its nodes characterized by the partial Euclidean distances (PEDs) as a metric. Each node in the ST is expanded to $|\Omega|$ child nodes, with $|\cdot|$ as the cardinality of a set, until the bottom level is reached. The accumulated PED at the a-th level, d_a, of the ST is

$$d_a = d_{a+1} + |e_a|^2, \tag{14}$$

where the distance increment $|e_a|^2 = |\tilde{y}_a - \sum_{b=a}^{m} r_{a,b}\dot{x}_b|^2$. It is important to recall that d_{m+1} is initiated with 0.

B. Using KBA in the ST

A drawback of (13) is the high complexity of the exhaustive search over the entire constellation space throughout the ST to reach the ML solution. As a result, some nodes in the ST with high accumulated PEDs can be rejected to save complexity without affecting the optimal performance. Hence, the KBA limits the search of (13) as

$$\begin{aligned} \hat{\mathbf{x}}_{\mathrm{KBA}} = \arg\min \Bigg(& |\tilde{y}_m - r_{m,m}\dot{x}_m|^2 + \left| \tilde{y}_{m-1} - \sum_{b=m-1}^{m} r_{m-1,b}\dot{x}_b \right|^2 \\ & + \cdots + \left| \tilde{y}_1 - \sum_{b=1}^{m} r_{1,b}\dot{x}_b \right|^2 \leq \rho^2_{\mathrm{KBA}} \Bigg) \\ & \text{s.t.} \quad \dot{x} \in \Omega, \end{aligned} \tag{15}$$

where ρ^2_{KBA} represents the threshold of the KBA to restrict the search space inside a specific radius. It is worth noting that ρ^2_{KBA} varies to guarantee that the proposed KBA visits only the lowest K nodes at each ST level. With a proper selection of K, the proposed KBA can achieve ML performance with a significant reduction in complexity.

Fig. 2 shows a numerical example of the proposed KBA for 4-QAM 2×2 MIMO RIS-ISAC system. In each level, only the smallest $K = 2$ nodes are expanded into 2 child visited nodes (VNs). Algorithm 1 summarizes the proposed KBA.

IV. Computational Complexity Analysis

The computational complexity of the proposed KBA generally depends on the number of VNs in the ST and the cost of obtaining each node in terms of the number of RA and RM. To determine the computational complexity of the KBA, the ST's levels are grouped into groups 1 and 2. In group 1, the number of VNs in each level, $VN_a^{\mathrm{KBA}} \leq K$, while $VN_a^{\mathrm{KBA}} > K$ for each level in group 2, as shown in Fig. 2. In light of [18], the number of VNs by the KBA for a given K and M is

$$C^{\mathrm{VN}}_{\mathrm{KBA}} = \sqrt{M}\left[\frac{1-(\sqrt{M})^{L+1}}{1-\sqrt{M}} + (m-L-1)K \right], \tag{16}$$

where $L = \lfloor \frac{\ln(K)}{\ln(\sqrt{M})} \rfloor$ is the number of levels in group 1 of the ST, with $\lfloor\cdot\rfloor$ as the floor operation. It can be observed that $0 \leq L \leq m$, depending on the value of K and M. The computational cost of each VN in terms of the number of RA and RM, respectively denoted by $C^{\mathrm{RA}}_{\mathrm{KBA}}$ and $C^{\mathrm{RM}}_{\mathrm{KBA}}$, are derived herein by grouping the range of L into three cases.

1) Case I ($L = 0$): Beyond the topmost level that always has $\sqrt{M}$ nodes, the cost of obtaining the nodes in the ST, if $L = 0$, is an arithmetic series of $K\sqrt{M}$ arising from the addition of the PEDs from the previous level. Thus, the number of RA and RM are respectively given by $C^{\mathrm{RA}}_{\mathrm{KBA}} = \sqrt{M} + \sum_{a=2}^{m}(a+1)K\sqrt{M}$, and $C^{\mathrm{RM}}_{\mathrm{KBA}} = \sqrt{M} + \sum_{a=2}^{m} aK\sqrt{M}$.

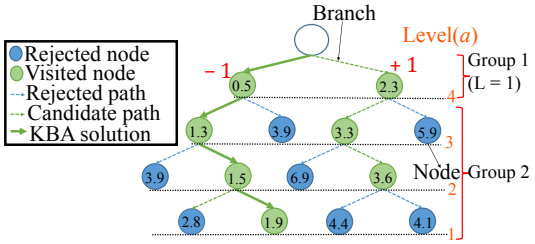

Fig. 2: Numerical example for the proposed KBA of a 4-QAM 2×2 MIMO RIS-ISAC system using $K = 2$.

2) Case II ($0 < L \leq m-2$): Each node in the topmost L levels is expanded to $\sqrt{M}$ child nodes. If $L \leq m-2$, every VN is expanded to $\sqrt{M}$ child nodes until the ST reaches the $(L+1)$-th level. From the $(L+2)$-th level to the bottom of the ST, the complexity takes the same form as Case *I*. In this case, the computational complexities are $C_{\text{KBA}}^{\text{RA}} = \sqrt{M} + \sum_{a=2}^{L+1}(a+1)M^{\frac{a}{2}} + \sum_{a=L+2}^{m}(a+1)K\sqrt{M}$, and $C_{\text{KBA}}^{\text{RM}} = \sqrt{M} + \sum_{a=2}^{L+1} aM^{\frac{a}{2}} + \sum_{a=L+2}^{m} aK\sqrt{M}$.

3) Case III ($L \geq m-1$): This case includes the realization of ML detection by the ST. In this instance, each node is expanded until the bottom of the ST is reached. Thus, the number of VNs increases exponentially as the ST is traversed from top to bottom. The computational costs for this case are $C_{\text{KBA}}^{\text{RA}} = \sqrt{M} + \sum_{a=2}^{m}(a+1)M^{\frac{a}{2}}$, and $C_{\text{KBA}}^{\text{RM}} = \sqrt{M} + \sum_{a=2}^{m} aM^{\frac{a}{2}}$.

In summary,

$$C_{\text{KBA}}^{\text{RA}} = \begin{cases} \sqrt{M} + \sum_{a=2}^{m}(a+1)K\sqrt{M}, & \text{if } L = 0 \\ \sqrt{M} + \sum_{a=2}^{L+1}(a+1)M^{\frac{a}{2}} + \\ \sum_{a=L+2}^{m}(a+1)K\sqrt{M}, & \text{if } 0 < L \leq m-2 \\ \sqrt{M} + \sum_{a=2}^{m}(a+1)M^{\frac{a}{2}}, & \text{if } L \geq m-1 \end{cases} \tag{17}$$

and

$$C_{\text{KBA}}^{\text{RM}} = \begin{cases} \sqrt{M} + \sum_{a=2}^{m} aK\sqrt{M}, & \text{if } L = 0 \\ \sqrt{M} + \sum_{a=2}^{L+1} aM^{\frac{a}{2}} + \\ \sum_{a=L+2}^{m} aK\sqrt{M}, & \text{if } 0 < L \leq m-2 \\ \sqrt{M} + \sum_{a=2}^{m} aM^{\frac{a}{2}}, & \text{if } L \geq m-1 \end{cases} \tag{18}$$

The amount of complexity saved by the proposed KBA compared to the complexity of ML detection is expressed as

$$C_{saved} = \left(1 - \frac{C_{\text{KBA}}}{C_{\text{ML}}}\right) \times 100. \tag{19}$$

V. Numerical Results

This section presents numerical results illustrating the communication and sensing performances of the RIS-ISAC system, in terms of bit-error rate (BER) and MSE respectively, using Monte Carlo simulation. The parameters used in simulation are: $N_{ts} = N_{tu} = N_r = 4$, and SINR_C is varied within the range of -15 to 30 dB. $\mathbf{F}$ and $\mathbf{G}$ are both modeled as Rician fading channels with a Rician factor, $K_{\text{dB}} = 7$ dB. The performance of the proposed KBA is compared with that of the ML detector, as an optimum benchmark.

Figs. 3(a) and 3(c) illustrate the variation in the BER and MSE performances for the proposed KBA at $N = 10$. When

Algorithm 1 Pseudo-Code of the Proposed KBA

Reserve $\mathbf{d} = [\cdot]$ to store the node metrics.
Initialize root node with metric $d_{m+1} = 0$.
for $a = m : -1 : 1$ **do**
  if $a = m$ **then**
    Compute $\mathbf{d}_a = |\tilde{y}_a - r_{a,a}x|^2 + d_{a+1}, \forall x \in \Omega$.
  else
    for $k = 1 : \min(K, |\Omega|)$ **do**
      Expand the $\min(K, |\Omega|)$ survived nodes from the $(a+1)$-th level to $|\Omega|$ child nodes each.
      Compute

$$\mathbf{d}_a = \left|\tilde{y}_a - (r_{a,a}x + \sum_{b=a+1}^{m} r_{a,b}\hat{x}_{b,k})\right|^2 + \mathbf{d}_{v_{\text{best}}}(k), \forall x \in \Omega.$$

    end for
  end if
  Determine the number of child nodes at level a:

$$\text{nodes} = \text{numel}(\mathbf{d}_a)$$

  Sort $\mathbf{d}_a$ in ascending order as: $[\mathbf{d}_v, \mathbf{d}_i] = \text{sort}(\mathbf{d}_a)$.
  Select the K least path metric nodes as:

$$\mathbf{d}_{v_{\text{best}}} = \mathbf{d}_v(1 : \min(K, \text{nodes})).$$

  Set $\hat{\mathbf{x}}_a \rightarrow \Omega\{\mathbf{d}_i(1 : \min(K, \text{nodes})\}$.
  Update the path history of $\hat{\mathbf{x}}_a$.
end for
Estimate $\hat{\mathbf{x}}_{\text{KBA}}$ from $\hat{\mathbf{x}}_{\text{KBA}} = \hat{\mathbf{x}}_{a(\min(\mathbf{d}_{v_{\text{best}}}))}$.

$K = 1$, the BER is significantly higher than the ML. As K increases, there is an exponential decrease in BER, aligning closely with the ML performance at $K = 5$, as depicted in Fig. 3(a). This alignment is further verified by Fig. 3(b) for different values of SINR_C. Two behavioral regions are apparent in Fig. 3(c). At low SINR_C, $\sqrt{P_c}$ in (8) significantly contributes to the rise in the MSE of estimating ζ. Once SINR_C surpasses a certain value, there is a notable decline in the MSE due to Δ in (8) approaching zero. It can be seen from Fig. 3(d) that the proposed KBA achieves identical BER results to that of ML detection at different M and SINRs, indicating the KBA's applicability for higher modulation orders.

Fig. 4 shows the BER and MSE performances for $N = 0, 10,$ and 20. As illustrated in Fig. 4(a), the BER improves with N due to the RIS providing multiple signal replicas through LoS and multipath components, enhancing system diversity and symbol detection accuracy. The MSE behaves differently across regions of SINR_C. At low SINR_C, smaller N values yield minimal MSE, mainly affected by $\mathbf{H}$ as outlined in 8. As N increases, the MSE initially rises due to errors from the enhanced channel matrix, but at higher SINR_C and improved BER, the MSE for $N = 20$ shows a rapid decrease, surpassing the performance of $N = 0$. This trend suggests that increasing the number of reflecting elements significantly improves BER and MSE as SINR_C rises, owing to the virtual LoS paths created by the RIS.

The computational complexity gain attained by the proposed KBA is shown in Fig. 5 in terms of VNs, RA, and RM. The comparative computational complexity analysis indicates that with $K = 5$, the algorithm reaches close to ML performance,

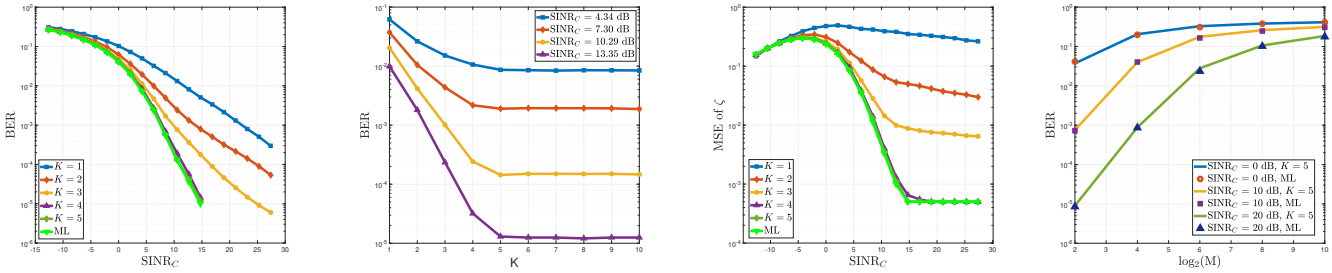

(a) BER vs. SINR$_C$ (b) BER vs. K (c) MSE vs. SINR$_C$ (d) BER vs. M

Fig. 3: Performance comparison of the proposed MIMO RIS-ISAC system.

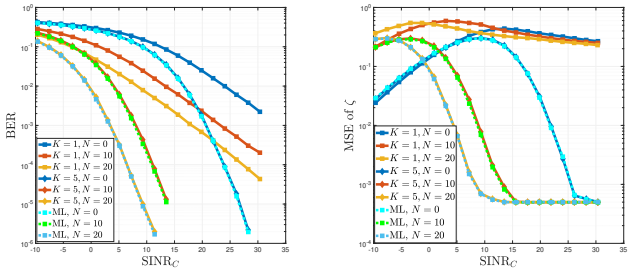

(a) BER vs. SINR$_C$ (b) MSE vs. SINR$_C$

Fig. 4: BER and MSE vs. SINR$_C$ for the MIMO RIS-ISAC.

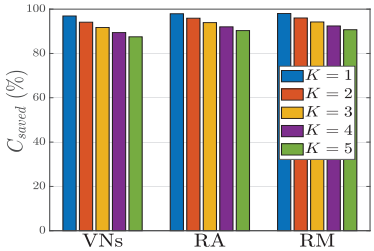

Fig. 5: Complexity saving by the proposed KBA.

resulting in substantial savings of 87%, 90.3%, and 90.7% in VNs, RA, and RM, respectively. One of the key advantages of the proposed KBA is its flexibility due to the trade-off between complexity and BER, as seen in Fig. 3 and Fig. 5. Thus, in practical scenarios requiring a target BER, selecting a lower value of K can further reduce computational complexity. This capability makes the proposed KBA beneficial for systems prioritizing efficiency without compromising performance.

VI. Conclusion

This letter investigated a MIMO RIS-ISAC system. The RIS was introduced to enhance the communication channel and improve the BER performance. The received signal equation was reformulated to employ the ST to decode the communication signal. Moreover, the KBA was proposed and studied for the MIMO RIS-ISAC system. It was observed that the KBA achieves near-ML performance with about 90% less complexity. Also, the proposed KBA demonstrated a desirable trade-off between complexity and performance, making it suitable for practical systems. By increasing the value of K, the proposed algorithm showed improved BER performances at increasing complexities. The IC-based MMSE technique was adopted to estimate the target's reflection coefficients in the MIMO RIS-ISAC system after detecting the communication signal. It was found that at low communication SINR, the introduction of the RIS improved the BER at the expense of the estimator's MSE. The latter was due to the increased error propagation during the IC-based estimation. Future work could investigate the dynamic selection of K for a variety of initialized systems and improved target coefficient estimation techniques.

References

[1] F. Liu *et al.*, "Integrated sensing and communications: Toward dual-functional wireless networks for 6G and beyond," *IEEE J. Sel. Areas Commun.*, vol. 40, no. 6, pp. 1728–1767, Mar. 2022.

[2] M. A. ElMossallamy *et al.*, "Reconfigurable intelligent surfaces for wireless communications: Principles, challenges, and opportunities," *IEEE Trans. Cogn. Commun. and Netw.*, vol. 6, no. 3, pp. 990–1002, May 2020.

[3] Y. Liu *et al.*, "Reconfigurable intelligent surfaces: Principles and opportunities," *IEEE Commun. Surv. Tuts.*, vol. 23, no. 3, pp. 1546–1577, May 2021.

[4] H. Luo *et al.*, "Joint beamforming design for RIS-assisted integrated sensing and communication systems," *IEEE Trans. Veh. Technol.*, vol. 71, no. 12, pp. 13 393–13 397, Aug. 2022.

[5] Q. Zhu *et al.*, "Joint transceiver beamforming and reflecting design for active RIS-aided ISAC systems," *IEEE Trans. Veh. Technol.*, Feb. 2023.

[6] H. Zhang, "Joint waveform and phase shift design for RIS-assisted integrated sensing and communication based on mutual information," *IEEE Commun. Lett.*, vol. 26, no. 10, pp. 2317–2321, Jul. 2022.

[7] X. Wang *et al.*, "Joint waveform and discrete phase shift design for RIS-assisted integrated sensing and communication system under Cramer-Rao bound constraint," *IEEE Trans. Veh. Technol.*, vol. 71, no. 1, pp. 1004–1009, Oct. 2021.

[8] M. Li *et al.*, "STAR-RIS aided integrated sensing and communication over high mobility scenario," *IEEE Trans. Commun.*, vol. 72, no. 8, pp. 4788–4802, Aug. 2024.

[9] Y. Dong, F. Liu, and Y. Xiong, "Joint receiver design for integrated sensing and communications," *IEEE Commun. Lett.*, vol. 27, no. 7, pp. 1854–1858, May 2023.

[10] M. Elsayed *et al.*, "Machine learning-based self-interference cancellation for full-duplex radio: Approaches, open challenges, and future research directions," *IEEE Open J. Veh. Technol.*, vol. 5, pp. 21–47, Nov. 2023.

[11] R. Liu *et al.*, "Integrated sensing and communication with reconfigurable intelligent surfaces: Opportunities, applications, and future directions," *IEEE Wireless Commun. Lett.*, vol. 30, no. 1, pp. 50–57, Feb. 2023.

[12] I. Al-Nahhal *et al.*, "Reconfigurable intelligent surface optimization for uplink sparse code multiple access," *IEEE Commun. Lett.*, vol. 26, no. 1, pp. 133–137, 2022.

[13] M. Richards, *Fundamentals of Radar Signal Processing*. McGraw-Hill Education, 2014.

[14] J. A. Zhang *et al.*, "An overview of signal processing techniques for joint communication and radar sensing," *IEEE J. Sel. Topics Signal Process.*, vol. 15, no. 6, pp. 1295–1315, Sep. 2021.

[15] Z. Guo and P. Nilsson, "Algorithm and implementation of the K-best sphere decoding for MIMO detection," *IEEE J. Sel. Areas Commun.*, vol. 24, no. 3, pp. 491–503, Mar. 2006.

[16] Q. Li and Z. Wang, "Improved K-best sphere decoding algorithms for MIMO systems," in *Proc. IEEE ISCAS*, May 2006, pp. 1159–1162.

[17] M. Shabany, K. Su, and P. Glenn Gulak, "A pipelined scalable high-throughput implementation of a near-ML K-best complex lattice decoder," in *Proc. IEEE Int. Conf. Acoust. Speech Signal Process.*, Mar. 2008, pp. 3173–3176.

[18] I. Al-Nahhal *et al.*, "Reduced complexity K-best sphere decoding algorithms for ill-conditioned MIMO channels," in *Proc. IEEE Annu. Consum. Commun. Netw. Conf.*, Jan. 2016, pp. 183–187.